Skeletal muscle lipidomics as a new tool to determine altered lipid homeostasis in fish exposed to urban and industrial wastewaters

Anna Marqueño[1], Maria Blanco[1], Alberto Maceda-Veiga[2], Cinta Porte[1*]

[1]Environmental Chemistry Department, IDAEA-CSIC, Jordi Girona 18, 08034 Barcelona, Spain.

[2]Department of Evolutionary Biology, Ecology and Environmental Sciences - IRBio, Faculty of Biology, University of Barcelona, 08028 Barcelona, Spain

***Corresponding author:** Cinta Porte

e-mail: cpvqam@cid.csic.es

Abstract

This work applies ultra-high performance liquid chromatography coupled to high-resolution mass spectrometry (UPLC-HRMS) to characterize for the first time the lipidome of the skeletal muscle of two fish species (*Barbus meridionalis*, *Squalius laietanus)* collected in a Mediterranean River affected by urban and industrial wastewater outflows. The untargeted analysis allowed a clear separation of the lipidome of fish from polluted and reference sites; phosphatidylcholines (PCs), phosphatidylethanolamines (PEs) and their lyso and ether-linked forms were among the distinctive features. The targeted analysis consistently detected a decrease in PC-plasmalogens (36:4, 36:6, 38:6) and highly unsaturated PCs (36:5, 36:6, 38:6, 40:6, 40:7), and an increase in plasmanyl-PCs (36:5, 38:5), lyso-PCs (16:1, 18:1, 22:4) and cholesteryl esters (CEs) (16:0, 18:0, 20:4) in fish from polluted sites. These lipid profiles were indicative of oxidative stress and dysregulation of cholesterol homeostasis in fish from polluted sites. This methodology represents a promising tool for the development of novel non-invasive diagnostic methods based on muscle tissue biopsies to assess the effects of water pollution in wildlife.

Keywords: Pollution, fish, lipidomics, LC-MS, XCMS online, targeted, untargeted

INTRODUCTION

Recent advances on mass spectrometry have allowed the characterization of complex lipidomes of tissues, cells and biofluids, and have been applied successfully in the investigation of human diseases and in the development of biomarkers of cancer, inflammation and neuropathic diseases.[1] However, lipidomic profiling has rarely been applied to investigate environmental disturbances and the response to environmental stressors in aquatic organisms, where lipids are involved in many essential biological functions, including signal transduction, hormonal regulation, energy balance and cell-signalling.[2,3] Natural factors, including temperature, nutrition, aging, reproduction, but also exposure to pollutants (e.g. endocrine disrupters) may alter lipid metabolism and, consequently, lipid composition.[4] Indeed, Grün and Blumberg[5] pointed out at the existence of some chemicals, termed obesogens, which disregulated lipid metabolism and promoted adipogenesis in murine preadipocytes. Since then, the obesogenic properties of tributyltin (TBT), and the ability of phthalates, bisphenol A (BPA) and BPA analogues, among others, to interfere with lipid metabolism in fish have been described.[6] However, these studies were performed in captive-reared animals or isolated tissues and cells exposed to single compounds, while evidences of lipid disruption in wild organisms exposed to a combination of natural and anthropogenic stressors are still few.[7]

Freshwater scarcity affects two thirds of the world's population, and half a billion people face severe water shortages throughout the year.[8] Rivers from semi-arid regions, like many Mediterranean rivers, exemplify this problem by being aquatic ecosystems with low water flow and often, poor water quality. During the dry seasons, these rivers receive urban and industrial effluents with a very low dilution factor and

experience a significant reduction of water quality.[9] Fish, which are good indicators of river health, are among the most affected taxa. The decline of riverine fish diversity throughout the world, and the decrease of native cyprinids in the northeast of Spain in particular, are examples of this situation.[10] In a previous study, we investigated the health status of these two cyprinids (*Barbus meridionalis* and *Squalius laietanus*) in a Mediterranean river (Ripoll River) after a major investment in sewage treatment plants (STPs) and restoration policies. Although the water quality and ecological state of the river improved substantially, fish collected in areas affected by STP effluents showed exposure to metals, alkylphenols and other organic pollutants, along with induction of liver enzymes, endocrine alterations and genotoxic effects.[9,11] Certainly, urban and industrial wastewater effluents are a major source of endocrine disruptors in the aquatic environment; they cause significant alterations of the endocrine system in exposed organisms and, often reproductive impairement.[12] The endocrine system plays a fundamental role in the regulation of the metabolism of lipids, carbohydrates and proteins, and any alteration of the endocrine system can lead to an imbalance of these hormonally driven processes, including changes in the metabolome and lipidome of the exposed organisms.[4,6]

Thus, here we examine the lipid profile of a small portion of the white skeletal muscle of two native fish species (*B. meridionalis* and *S. laietanus*) collected along a highly impacted Mediterranean river by using both, untargeted and targeted lipidomic approaches. By building on a previous study,[11] our main objective was to investigate if it is possible to discriminate between the lipidome of fish exposed to STP effluents from those collected at reference sites and, if so, to discuss the potential that lipidomics has for environmental wildlife monitoring, through the development of new biomarkers of fish health status.

MATERIAL AND METHODS

Chemicals. LC-MS grade water (≥ 99%) and methanol (≥ 99%) were from Merck (Darmstadt, Germany). Nitrogen (purity > 99.999%) supplied by Air Liquide (Madrid, Spain) was used for the ESI source. Formic acid was purchased from J.T. Baker® (Deventer, Netherland) and ammonium formate (≥ 99.0%) was from Sigma Aldrich. Lipid standards, namely 16:0 D31-18:1 phosphatidylcholine (16:0 D31-18:1 PC), 17:0 lyso-PC (17:0 LPC), 16:0 D31-18:1 phosphatidylethanolamine (16:0 D31-18:1 PE), 16:0 D31-18:1 phosphatidylserine (16:0 D31-18:1 PS), 16:0 D31-18:1 phosphatidic acid (16:0 D31-18:1 PA), 16:0 D31-18:1 phosphatidylinositol (16:0 D31-18:1 PI), 16:0 D31-18:1 phosphatidylglycerol (16:0 D31-18:1 PG), 1,2,3-17:0 triglyceride (1,2,3-17:0 TG), 1,3-17:0 D5 diglyceride (1,3-17:0 D5 DG) and 17:0 cholesteryl ester (17:0 CE), were from Avanti Polar Lipids (Alabaster, AL, USA).

Sample collection. Sampling sites were selected following a pollution gradient to include upstream reference sites (R1, R2, R3), and downstream areas, affected by urban and industrial wastewater effluents (P1, P2, P3) in the Ripoll River. Two STP, treating approximately 30,000 $m^3 \cdot day^{-1}$, are located in P1 and P3 (Figure S1, supplementary information). The maximum flow of the river is of 4,800 $m^3 \cdot day^{-1}$ in summer. Over the sampling period (July 2012), STP effluents mainly determined the river flow. Fish (*B. meridionalis* and *S. laietanus*) were sampled with a portable electrofishing unit by following an international standardized fish sampling method (CEN standards EN 14962 and EN 14011). Immediately after collection, a small piece of the white skeletal muscle (0.2-0.3 g) was dissected below the dorsal fin, frozen in liquid nitrogen and stored at -80 ºC.[11]

Lipid analysis. The muscle sample was homogenized and a subsample (20 mg) was taken per fish; four different individuals were pooled and freeze-dried. Three pools made of different fish were prepared per sampling site, so that 12 individuals per site were analyzed. Lipids were extracted (5 mg freeze-dried tissue) with methanol:chloroform (1:2) containing 0.01% of butylated hydroxytoluene (BHT) in an ultrasonic bath for 5 min (x2) after the addition of 200 pmol of the internal standard mix.[13]

To identify plasmanyl-PC (PC-O) and plasmalogen-PC (PC-P) isomeric species, a group of extracts were derivatized right before analysis as described in Lydic et al.[14] Briefly, a daily-prepared solution of 0.4 mM iodine in chloroform was mixed with 6 mM ammonium bicarbonate in methanol (2:1); 500 µL of the resulting mixture were added to the dry lipid extracts, and incubated for 5 minutes in an ice bath. The extracts were evaporated under nitrogen and reconstituted in methanol for injection. Under these conditions, the plasmalogen species containing an alkenyl double bound are hydrolyzed and only the alkyl forms are detected in the chromatograms of the derivatized samples.

Lipid extracts were injected in a ultrahigh performance liquid chromatography (UHPLC) Waters Acquity UHPLC system fitted with a 100 mm x 2.1 mm id, 1.7 µm C8 Acquity UPLC BEH column (Waters, Ireland), which was coupled to a Waters LCT Premier XE Time of Flight Mass Spectrometer (Waters, Millford, MA), operated in positive electrospray ionization mode (ESI+)[15]. Full scan spectra from 200 to 1000 Da were obtained. Mass accuracy and reproducibility were maintained by using an independent reference spray via LockSpray. The mass resolving power of the ToF-HRMS (determined from the $[M+H]^+$ ion of leucine at m/z 556.2771) was 10,000 FWHM (full with at half maximum). The capillary voltage was 3.0 kV, with a

desolvation temperature of 350ºC and a desolvation gas flow of 600 $L \cdot h^{-1}$. The mobile phases were 1 mM ammonium formate in methanol (phase A) and 2 mM ammonium formate in H_2O (phase B), both phases with 0.2% of formic acid. The programmed gradient was: 0 min, 80% A; 3 min, 90% A; 6 min, 90% A; 15 min, 99% A; 19 min, 99% A; 21 min, 80% A held for 2 min. The flow rate was 0.3 mL/min and the injection volume was 8 µL.

Untargeted analysis. The data was processed with an untargeted approach using the XCMS online platform to detect the most dysregulated features between samples P and R. Raw data was converted to mzXML using MSConvert and further analyzed by using pairwise job on the web interface XCMS. *CentWave* was the algorithm used for feature detection using 30 ppm as the maximum *m/z* deviation tolerated, and a range of 2 to 25 seconds for the chromatographic peak widths. As prefiltering, mass traces were only retained if they contained at least 3 peaks with intensities equal or greater than 1000, with a signal to noise threshold higher than 6. The *obiwarp* algorithm was chosen for retention time correction. For the alignment of the chromatograms, a deviation of 5 seconds in the retention time was allowed, whilst 0.025 amu was selected as width of overlapping in *m/z* slices, and 0.5 was the minimum fraction of samples necessary within a sampling class (P or R) to be valid group.

Targeted analysis. Data was also analysed using suspected targeted screening. A home-made referential lipid database was built by obtaining theoretical exact masses using a spectrum simulation tool of MassLynx software and LIPID MAPS online database, obtaining an inventory of lipids, including PC, PC-O, PC-P, LPC, TG, DG, CE and, sphingomyelin (SM). Lipids were identified under the criteria of accurate mass

measurement (error < 5 ppm) and isotopic distribution. Individual peaks were isolated from full-scan MS spectra and a list of candidates for that specific exact mass was generated by formula determination tool (Micromass MassLynx softwate). Quantification was carried out using the corresponding extracted ion chromatograms; the linear dynamic range was determined by injection of standard mixtures. Lipid species belonging to a specific lipid subclass were referred to different internal standards. Thus, TGs were referred to 1,2,3-17:0 TG; DGs to 1,3-17:0 D5 DG; PCs, PC-Os, PC-Ps and SMs to 16:0 D31-18:1 PC; CEs to 17:0 CE; and LPCs to 17:0 LPC. Repeatability expressed as intra-day relative standard deviation (RSD) calculated for all lipid standards relative abundance in the samples, was lower than 30% in all cases (TG: 26%, DG: 21%, PC: 13%, LPC: 12%).

Statistical analysis. A multivariate statistical analysis was performed using the XCMS online platform[16] to study whether the muscle of fish from polluted sites presented a differential signature in their lipid profile. A principal component analysis (PCA) was firstly performed, followed by the generation of a heatmap to show up/down regulation of the detected features. Finally, a cloud plot that shows data characteristics such as retention time, mass-to-charge ratio, signal intensity of features, fold change and *p*-value (Welch *t* test), was used to visualize the ion features causing the group segregation. For the targeted analysis, multivariate and univariate approaches were applied using the online software Metaboanalyst 4.0.[17] Data was normalized by sum and autoscaled. First, unsupervised principal component analysis (PCA) of the dataset was performed to explore differences of the lipid profiles between reference and polluted sampling sites. After, partial least square-discriminant analysis (PLS-DA) was performed in order to obtain the maximum segregation between lipid profiles of fish

collected in the different stations. Heatmap cluster analysis for the lipids of interest (variables important in projection (VIPs) > 1.0) was used to arrange lipids according to similarity and to retain the more contrasting variables. Finally, volcano plots were applied to visualize the significance and the magnitude of the changes detected in the lipidome of fish from P and R sites (fold change ≥ 1.5/2.0; $p < 0.05$, Student *t*-test).

RESULTS AND DISCUSSION

Differential exposure. Size, weight and condition factor of the sampled individuals of *B. meridionalis* and *S. laietanus* are summarized in Table S1 (Supporting Information, SI). Water parameters (dissolved oxygen, temperature) were consistent across all the sampling sites; although, higher conductivity was detected in P sites.[11,] Biliary levels of organic pollutants (viz. naphthol, galaxolide, alkylphenols) and induction of the hepatic CYP1A and CYP3A catalysed activities were detected in *B. meridionalis* and *S. laietanus* collected downstream of STPs, indicating significant exposure to urban and industrial pollutants together with metabolic and endocrine alterations, and a differential exposure pattern in fish from P and R sites (Table S2, SI).

Untargeted analysis. The pre-processing of chromatograms of *B. meridionalis* and *S. laietanus* lipid extracts using XCMS online platform reported the detection of 659 and 641 features, respectively. PCA scores plot explained up to 39 and 41% of the variance, with good segregation of polluted and reference site samples (Figure 1A-B). Some features clearly differentiated samples from R and P sites, indicating a specific lipidomic signature in the muscle of fish collected in those areas. The cloud plot highlighted 117 (*B. meridionalis*) and 104 (*S. laietanus*) features that were significantly different among the groups (fold change ≥ 1.5; p-value ≤ 0.01) (Figure 2). The major part of altered features were found between 3 and 12 minutes, area of the chromatogram where phospholipids and lyso-phospholipids are eluted For retention times between 14 and 20 minutes (region of the chromatogram where TGs, DGs and CEs elute), the number of dysregulated features was comparatively low. Some up-regulated features were detected in *B. meridionalis* (Fig. 2A), while no features were observed in this region for *S. laietanus* (Fig. 2B). This may indicate a low sensitivity of the XCMS platform for sterol lipids and triglicerides (low intensity ions), but also no significant alteration of these lipid subclasses, particularly in *S. laietanus*.

For further filtering of the selected features, only the lipids formed by fatty acids with an even number of carbons and the most probable adducts formed during ionization ($[M+H]^+$, $[M+NH4]^+$), detected after analysis of the internal standards, were kept. The tentative identification of the different dysregulated features indicated PCs, PEs, PIs, PSs, PAs, PGs, CEs, SM, Cer (ceramides) and ether and lyso forms of the mentioned phospholipids, as the compounds that allowed a significant differentiation of the skeletal muscle lipidome of fish from P and R sites (Excel,SI).

Targeted analysis. Individual lipid species unresolved in the total ion chromatogram were successfully isolated when selecting their exact masses. PC, PC-O, PC-P and SM were the first lipid subclasses to elute and appeared in the initial 10 min span of the chromatogram. These lipids were totally resolved from DG, TG and CE which eluted in the subsequent 15-20 min. TG, DG and CE were mainly detected as ammonium adducts $[M+NH_4]^+$, whereas the rest of lipids were identified in the protonated form, $[M+H]^+$. About 119 lipids, including PC, PC-O, PC-P, LPC, CE, TG, DG and, SM were identified under the criteria of molecular formula, accurate mass with an error < 5 ppm, retention time and isotopic distribution (Table S3 SI). Quantitative analysis of the detected lipids evidenced that the most abundant lipids in muscle tissue of *B. meridionalis* from R sites were PCs representing 49% of the lipids analyzed, with PC 34:1, 36:5, 38:6 as the most abundant species. LPCs represented 22% of the lipids analyzed, being LPC 20:5 almost half of the LPCs content. TGs were the third more abundant group (18%) being TG 50:2 the most abundant species.

Likewise, PCs were the most abundant lipids in *S. laietanus* from R sites representing 39% of the lipids analyzed; the most abundant PC species were similar to those reported for *B. meridionalis*. TGs were also very abundant (31% of lipids analyzed), particularly TGs 52:2, 50:2, 52:3 and 50:1; followed by LPCs (20%), being LPC 20:5 and 18:1 the predominant ones. The rest of lipid subclasses represented less than 5% of lipids analyzed in both species (SI Table S3).

The PCA score plot of the lipidomic profile of *B. meridionalis* collected in the different sampling sites, resulted in a model with 3 principal components, which explained 70% of the variance (SI, Figure S2A). The plot displayed a good separation between P and R sites by PC2, demonstrating the significant changes of lipids depending on the sampling site. Partial least squares-discriminant analysis (PLS-DA) of

B. meridionalis lipidome explained 47% of the covariance (R^2: 0.89, Q^2: 0.79) within sampling sites (Figure 3A). The scores plot differentiated P sites, with no evident segregation among them, from R sites. Within R sites, only R3, the most upstream station, was completely resolved. From the PLS-DA, 50 VIP scores > 1.0 were generated. Among the up-regulated variables in P sites, PC-Os (30:0, 32:0/1, 34:1, 36:5, 38:5/6), some saturated and poorly unsaturated PCs (32:0-1, 34:0/2/3, 38:0/2, 36:1), and CEs (16/18:0) were found, while a decrease of LPC 20:5, PC-P 34:1 and PC 36:6 was detected. The heatmap cluster analysis based on the selection of VIPs > 1.0, grouped reference and polluted sites separately, despite no clear clustering within the polluted stations (Figure 4A). High levels of unsaturated TGs were observed in the lipidome of *B. meridionalis* from R3, while LPCs 20:4,5, PC 36:6 and SM 24:2 were accumulated in all reference sites.

Similarly, PCA score plot explained 71% of the variance with 3 principal components and showed a segregation of the lipid profile of *S. laietanus* with sampling sites (SI, Figure S2B). P sites were located in the upper quadrant of PC2 while most of the R samples were located in the lower quadrant. PLS-DA explained up to 54% of the covariance (R^2: 0.89, Q^2: 0.60) (Figure 3B) for *S. laietanus*. It showed a segregation between P and R sites, although P sites were not resolved between them, while for R sites, only R1 was successfully segregated from R2 and R3. R1 corresponds to the reference site located closer to P sites along the river, being the closest to polluted sites in the PLS-DA. 41 VIP scores > 1.0 were generated from PLS-DA, evidencing high levels of PC 30:0, LPCs with low number of double bonds (16:1, 18:1/2, 20:1/2), PC-Os (30:0, 32:1, 34:1, 36:1/5, 38:5), and a decrease of SM 16:1 and unsaturated PCs (34:3, 36:4/5/6, 38:5/6, 40:5) in P stations. The heatmap cluster analysis allowed a clear

observation of the dysregulated lipids; most samples were grouped into two differentiated clusters corresponding to R and P sites.

Since for both fish species, the cluster analysis arranged separately polluted and reference areas, P and R sites were grouped for further analysis with a volcano plot (Figure 5). When setting a fold change ≥ 2.0 and *p*-value < 0.05, the lipidome of *B. meridionalis* from P sites was characterized by low levels of PC 40:5 and PC-P 36:2/4, and an accumulation of PC-O 32:0, 36:5, 38:5, LPC 18:2, 20:2, CE 18:0/2, 20:4 and PC 34:0, 36:3. When a lower fold change was set (fold change ≥ 1.5), the lipid subclasses suffering dysregulation did not vary, but increased the number of lipid species.

In contrast, very few lipids showed a fold-change > 2.0 (*p*-value < 0.05) when comparing the lipidome of *S. laietanus* from P and R sites. Mainly, an accumulation of LPC 20:1/2, 22:4 and a reduction of PC 36:6 was observed in P sites. In order to observe the more subtle lipid changes, the fold change was set to ≥ 1.5, an increment of the number of LPC species up-regulated was detected, together with an increase of PC-Os 32:0/1, 34:1, CEs 20:1/4 and TG 50:0, and a concomitant decrease of highly unsaturated PCs, DGs (34:3, 36:4/5) and SM 16:1.

The combined application of the untargeted and targeted approach to investigate the lipidome of the skeletal muscle of *B. meridionalis* and *S. laietanus* provided complementary information. The untargeted strategy evidenced a clear segregation of the lipidome of fish inhabiting areas impacted by wastewater effluents in comparison to individuals sampled at reference sites. Some of the down-regulated features were putatively identified as long chain highly unsaturated fatty acid phospholipids, whilst a number of features exhibiting up-regulation were identified as saturated or poorly unsaturated phospholipids (from one to four double bounds) (SI Excel). An alteration on the composition of the lipids conforming the cellular membranes can have harmful

consequences, since polyunsaturated phospholipids confer higher melting point and fluidity to the membranes than saturated phospholipids, altering their structure and functionality.[18] The targeted analysis confirmed a decrease of PCs with a high number of double bonds (5-9) in individuals collected in P sites; this decrease was more evident for *S. laietanus*. Reactive oxygen species (ROS), generated as subproducts of normal metabolism, increased after exposure to different xenobiotics, as pharmaceuticals, personal care products, and other contaminants often detected in wastewater treatment plant effluents, and induced oxidative stress in fish.[19,20] In our study, 100 to 1000-fold higher levels of 2-naphthol, galaxolide and alkylphenols were detected in fish collected in P sites in comparison to R sites (Table S2, SI). Thus, we hypothesize that a greater exposure to pollutants (urban/industrial origin) may lead to increased generation of ROS and consequently, a higher oxidation of phospholipids containing PUFAs, which are the most susceptible to peroxidation and ROS attack.[21] This hypothesis is further supported by previous results observed in-vitro, where a general depletion of polyunsaturated lipids, namely PCs (36:5, 38:5, 38:6), PC-Ps and PEs/PE-Ps were detected both, in PLHC-1 and JEG-3 cells exposed to compounds that significantly induced the generation of ROS.[22]. However, other hypothesis like the reduced biosynthesis of highly unsaturated lipids in fish from polluted sites cannot be discarded.

Despite the comparatively lower exposure to xenobiotics of *Squalius laietanus*,[11] the decrease of highly unsaturated PCs (36:5,6; 38:5,6; 40:5) was more significant than in *B. mediterraneus* (PC 40:5). Interestingly, levels of PC-Ps were up to one order of magnitude higher in *B. meridionalis* than in *S. laietanus* (Fig. 6). Plasmalogens act as endogenous antioxidants because the vinyl-ether bond at the sn-1 position of the glycerol moiety makes them more susceptible to oxidative attack than other phospholipids.[23] Thus, plasmalogens function as scavengers by protecting other

phospholipids from oxidation,[24] and a deficiency of plasmalogens has been associated with increased lipid oxidation and an imbalance of the major lipid signaling pathways.[23] In consequence, the lower content of PC-Ps of *S. laietanus* would led to a higher susceptibility to oxidative stress and a comparatively higher depletion of highly unsaturated PCs in polluted sites.

Linked to the decrease of highly unsaturated PCs, a significant increase of LPCs was detected in the skeletal muscle of *S. laietanus.* Although no previous data has been obtained in fish, increased levels of LPCs are indicative of (a) increased hydrolysis of PCs by phospholipases in different vertebrate models[25,26] , and/or (b) increased activity of the enzyme lecithin:cholesterol acyltransferase, which catalyzes the transfer of the fatty acid of position sn-2 of phosphatidylcholine to free cholesterol, with formation of cholesterol esters and lysophosphatidylcholine.[27] Accordingly to these hypothesis, another characteristic feature of the fish collected at P sites was the enrichment of the skeletal muscle lipidome in cholesteryl esters. Cholesterol regulates cell membrane properties by maintaining sphingolipids rafts in a functional state, and it is a biosynthetic precursor of steroid hormones; therefore, levels of free cholesterol are tightly regulated through esterification and accumulation in cytosolic lipid droplets.[28] Exposure to metabolic disrupting compounds, including bisphenol A, phthalates and perfluoroalkyl substances, significantly altered cholesterol homeostasis in fish. Thus, bisphenol A upregulated mRNA expression of genes related to cholesterol metabolism, including acyl-coenzime A cholesterol acyltransferase, in marine medaka and zebra fish.[29,30] Phthalates and flame retardants increased the concentration of total cholesterol and triglycerides in gilthead sea bream hepatocytes.[31] Similarly, transcripts involved in cholesterol metabolism and mitochondrial function were altered in fathead minnows exposed to perfluoro alkyl substances,[32] and exposure to perfluorononanoic acid

increased cholesterol levels in the liver of zebra fish.[33] Also, tributyltin induced lipid accumulation and an increase in total cholesterol and triglycerides in muscle of rare minnows.[34] Accordingly to these observations, the muscle lipidome of *B. meridionalis* and *S. laietanus* collected in sites affected by urban and industrial wastewater outflows, was enriched in CEs. This increment of CEs is often accompanied by an induction of the synthesis of TGs.[30,31] However, in fish, adipose tissue is located in the intra-abdominal region, and not widely distributed through the body as in mammals,[6] thus, no significant enrichment of TGs was observed in the skeletal muscle of fish collected in P sites.

Additionally, the muscle lipidome of both, *B. meridionalis* and *S. laietanus* collected in polluted areas was enriched in PC-Os. PC-Os and PC-Ps are isobaric species but, while the function of the latter has been widely described, the functional role of PC-Os is not well understood. Increased levels of PC-Os have been reported in human tumor tissues[35] While the accumulation of PC-O selected species was present in the lipidome of both fish species from polluted sites, the increment was greater for *B. meridionalis*.

Overall, the number of significantly altered lipids highlighted by the volcano plots was higher for *B. meridionalis* than *S. laietanus*, suggesting a higher sensitivity of the former to endocrine and metabolic disrupters. This tendency was confirmed by the untargeted analysis, where a greater number of up-regulated features in P sites were obtained for *B. meridionalis*, and it is in agreement with our previous stuy[11], where *B. meridionalis* showed higher exposure to pollutants and higher sensitivity to estrogenic exposure than S. *laietanus*, an omnivorous water-column dweller, with greater resistance and adaptability to water pollution.[36]

Although the magnitude of the lipid changes was different for the two species examined, the fish collected at P sites showed some common alterations, which could be further investigated as potential biomarkers of exposure/impact of urban and industrial discharges, namely an enrichment in PC-Os, CEs and LPCs and a depletion of highly polyunsaturated PCs. Overall, this study demonstrates the potential of lipidomics approaches in toxicology and risk assessment studies to provide a specific signature of the impact of contaminants (e.g. oxidative stress, inflammation, metabolic disturbance). In addition, the applyed methodology represents a promising tool for the development of novel non-invasive monitoring methods based on muscle tissue biopsies.

Acknowledgments

Anna Marqueño acknowledges a pre-doctoral fellowship BES-2015-074842. Work financed by Ministerio de Ciencia e Innovación, under the project CGL2014-52144-P.

References

(1) Hu, C.; van der Heijden, R.; Wang, M.; van der Greef, J.; Hankemeier, T.; Xu, G. Analytical Strategies in Lipidomics and Applications in Disease Biomarker Discovery. *J. Chromatogr. B.* **2009**, *877* (26), 2836–2846.

(2) Tocher, D. R. Metabolism and Functions of Lipids and Fatty Acids in Teleost Fish. *Rev. Fish. Sci.* **2003**, *11* (2), 107–184.

(3) Tang, C.-H.; Shi, S.-H.; Lin, C.-Y.; Li, H.-H.; Wang, W.-H. Using lipidomic methodology to characterize coral response to herbicide contamination and develop an early biomonitoring model. *Sci. Total Environ.* **2019**, *648*, 1275–1283.

(4) Heindel, J. J.; Newbold, R.; Schug, T. T. Endocrine Disruptors and Obesity. *Nat. Rev. Endocrinol.* **2015**, *11*, 653.

(5) Grün, F.; Blumberg, B. Environmental Obesogens: Organotins and Endocrine Disruption via Nuclear Receptor Signaling. *Endocrinology.* **2006**, *147* (6), 50–55.

(6) Capitão, A.; Lyssimachou, A.; Filipe, L.; Castro, C.; Santos, M. M. Obesogens in the Aquatic Environment: An Evolutionary and Toxicological Perspective. *Environ. Int.* **2017**, *106*, 153–169.

(7) Melvin, S. D.; Lanctôt, C. M.; Doriean, N. J. C.; Bennett, W. W.; Carroll, A. R. NMR-based lipidomics of fish from a metal(loid) contaminated wetland show differences consistent with effects on cellular membranes and energy storage. *Sci. Total Environ.* **2019**, *654*, 284–291.

(8) Mekonnen, M. M.; Hoekstra, A. Y. Four billion people facing severe water scarcity. Sci. Adv. **2016**; 2 : e1500323.

(9) Maceda-Veiga, A.; Monroy, M.; Navarro, E.; Viscor, G.; de Sostoa, A. Metal Concentrations and Pathological Responses of Wild Native Fish Exposed to Sewage Discharge in a Mediterranean River. *Sci. Total Environ.* **2013**, *449*, 9–19.

(10) Maceda-Veiga, A. Towards the conservation of freshwater fish: Iberian Rivers as an example of threats and management practices. Rev. Fish Biol. Fisheries **2013**, *23*, 1-22.

(11) Blanco, M.; Rizzi, J.; Fernandes, D.; Colin, N.; Maceda-Veiga, A.; Porte, C. Assessing the Impact of Waste Water Effluents on Native Fish Species from a Semi-Arid Region, NE Spain. *Sci. Total Environ.* **2019**, *654*, 218–225.

(12) Petrie, B.; Barden, R.; Kasprzyk-Hordern, B. A review on emerging contaminants in wastewaters and the environment: Current knowledge, understudied areas and recommendations for future monitoring. *Water Res.* **2015,** *72*, 3-27.

(13) Christie, W. W. Rapid Separation and Quantification of Lipid Classes by High Performance Liquid Chromatography and Mass (Light-Scattering) Detection. *J. Lipid Res.* **1985**, *26*, 507–512.

(14) Lydic, T. A.; Townsend, S.; Adda, C. G.; Collins, C.; Mathivanan, S.; Reid, G. E. Rapid and Comprehensive "shotgun" Lipidome Profiling of Colorectal Cancer Cell Derived Exosomes. *Methods.* **2015**, *87*, 83–95.

(15) Gorrochategui, E.; Pérez-Albaladejo, E.; Casas, J.; Lacorte, S.; Porte, C. Perfluorinated chemicals: differential toxicity, inhibition of aromatase activity and alteration of cellular lipids in human placental cells. Toxicol. Appl. Pharmacol. **2014**, *277(2)*, 124-130.

(16) Gowda, H.; Ivanisevic, J.; Johnson, C. H.; Kurczy, M. E.; Benton, H. P.; Rinehart, D.; Nguyen, T.; Ray, J.; Kuehl, J.; Arevalo, B.; Westenskow, P.D.; Wang, J.; Arkin, A.P.; Deutschbauer, A.M.; Patti, G.J.; Siuzdak, G. Interactive XCMS Online: Simplifying Advanced Metabolomic Data Processing and Subsequent Statistical Analyses. *Anal. Chem.* **2014**, *86* (14), 6931–6939.

(17) Xia, J.; Wishart, D. S. Using Metaboanalyst 3.0 for Comprehensive Metabolomics Data Analysis. *Curr. Protoc. Bioinforma.* **2016**, *55*, 14.10.1-

14.10.91.

(18) Hashimoto, M.; Hossain, S. Fatty Acids: From Membrane Ingredients to Signaling Molecules. *In IntechOpen*. **2018**.

(19) Wu, M., Xu, H., Shen, Y., Qiu, W., Yang, M. Oxidative stress in zebrafish embryos induced by short-term exposure to bisphenol A, nonylphenol, and their mixture. *Environ. Toxicol. Chem.* **2011**, 30 (10), 2335–2341.

(20) Blaise, C., Andre, C., Gagne, F. Occurrence of pharmaceutical products in a municipal effluent and toxicity to rainbow trout (*Oncorhynchus mykiss*) hepatocytes. *Ecotoxicol. Environ. Saf.* **2006**, 64, 329–336.

(21) Łuczaj, W.; Gęgotek, A.; Skrzydlewska, E. Antioxidants and HNE in Redox Homeostasis. Free Radic. Biol. Med. 2017, 111, 87–101.

(22) Pérez-Albaladejo, E., Lacorte, S., Porte, C. Differential Toxicity of Alkylphenols in JEG-3 Human Placental Cells: Alteration of P450 Aromatase and Cell Lipid Composition. *Toxicol. Sci*. **2019**, 167 (2), 336–346.

(23) Braverman, N. E.; Moser, A. B. Functions of Plasmalogen Lipids in Health and Disease. *Biochim. Biophys. Acta.* **2012**, *1822* (9), 1442–1452.

(24) Brites, P.; Waterham, H. R.; Wanders, R. J. A. Functions and Biosynthesis of Plasmalogens in Health and Disease. *Biochim. Biophys. Acta - Mol. Cell Biol. Lipids.* **2004**, *1636* (2–3), 219–231.

(25) Koizumi, S.; Yamamoto, S.; Hayasaka, T.; Konishi, Y.; Yamaguchi-Okada, M.; Goto-Inoue, N.; Sugiura, Y.; Setou, M.; Namba, H. Imaging Mass Spectrometry Revealed the Production of Lyso-Phosphatidylcholine in the Injured Ischemic Rat Brain. *Neuroscience.* **2010**, *168* (1), 219–225.

(26) Kabarowski, J. H. G2A and LPC: Regulatory Functions in Immunity. *Prostaglandins Other Lipid Mediat.* **2009**, *89* (3–4), 73–81.

(27) Niu, J.; Liu, Y. J.; Tian, L. X.; Mai, K. S.; Yang, H. J.; Ye, C. X.; Zhu, Y. Effects of dietary phospholipid level in cobia (Rachycentron canadum) larvae: growth, survival, plasma lipids and enzymes of lipid metabolism. *Fish Physiol. Biochem.* **2008**, *34*, 9–17.

(28) Simons, K.; Ikonen, E. How Cells Handle Cholesterol. *Science.* **2000**, *290*, 1721–1727.

(29) Kim, B.; Jo, Y. J.; Lee, N.; Lee, N.; Woo, S.; Rhee, J.; Yum, S. Bisphenol A Induces a Distinct Transcriptome Profile in the Male Fish of the Marine Medaka *Oryzias javanicus*. *BioChip J.* **2018**, *12(1)*, 25–37.

(30) Santangeli, S.; Notarstefano, V.; Maradonna, F.; Giorgini, E.; Gioacchini, G.; Forner-piquer, I.; Habibi, H. R.; Carnevali, O. Effects of Diethylene Glycol Dibenzoate and Bisphenol A on the Lipid Metabolism of *Danio rerio*. *Sci. Total Environ.* **2018**, *636*, 641–655.

(31) Cocci, P.; Mosconi, G.; Palermo, F. A. Changes in Expression of MicroRNA Potentially Targeting Key Regulators of Lipid Metabolism in Primary Gilthead

Sea Bream Hepatocytes Exposed to Phthalates or Flame Retardants. *Aquat. Toxicol*. **2019**, *209*, 81–90.

(32) Rodríguez-Jorquera, I. A.; Colli-dula, R. C.; Kroll, K.; Jayasinghe, B. S.; Parachu Marco, M. V; Silva-Sanchez, C.; Toor, G. S.; Denslow, N. D. Blood Transcriptomics Analysis of Fish Exposed to Perfluoro Alkyls Substances: Assessment of a Non-Lethal Sampling Technique for Advancing Aquatic Toxicology Research. *Environ. Sci. Technol.* **2019**, *53*, 1441–1452.

(33) Zhang, W.; Zhang, Y.; Zhang, H.; Wang, J.; Cui, R.; Dai, J. Sex Differences in Transcriptional Expression of FABPs in Zebrafish Liver after Chronic Perfluorononanoic Acid Exposure. *Environ. Sci. Technol.* **2012**, *46*, 5175–5182.

(34) Zhang, J.; Zhang, C.; Ma, D.; Liu, M.; Huang, S. Lipid Accumulation, Oxidative Stress and Immune-Related Molecules Affected by Tributyltin Exposure in Muscle Tissues of Rare Minnow (*Gobiocypris rarus*). *Fish Shellfish Immunol.* **2017**, *71*, 10–18.

(35) Smith, R. E.; Lespi, P.; Di Luca, M.; Bustos, C.; Marra, F. A.; De Alaniz, M. J. T.; Marra, C. A. A Reliable Biomarker Derived from Plasmalogens to Evaluate Malignancy and Metastatic Capacity of Human Cancers. *Lipids*. **2008**, *43 (1)*, 79–89.

(36) Merciai, R.; Bailey, L. L.; Bestgen, K. R.; Fausch, K. D.; Zamora, L.; Sabater, S.; García-Berthou, E. Water Diversion Reduces Abundance and Survival of Two Mediterranean Cyprinids. *Ecol. Freshw. Fish*. **2018**, *27* (1), 481–491.

512 Figure 1. PCA scores plot of the skeletal muscle lipid extracts of A) *B. meridionalis* and
513 B) *S. laietanus* obtained with XCMS online platform after pairwise analysis comparing
514 polluted and reference sites.
515
516 Figure 2. Cloud plot for A) *B. meridionalis* and B) *S. laietanus* displaying the
517 dysregulated features ($p \leq 0.01$, fold change ≥ 1.5) in the skeletal muscle of fish from
518 polluted sites compared to reference sites. X axis represent retention time (min) while
519 *m/z* is displayed in the Y axis. Up-regulated features in polluted samples are shown in
520 green, down-regulated features in red. The size of the circles corresponds to the log-fold
521 change of that feature, while the shade of color is proportional to changes in *p* value
522 (high contrast colors belong to lowest *p* and vice-versa). Obtained using XCMS online
523 platform (pairwise analysis).
524
525 Figure 3. PLS-DA scores plot and first 25 highest ranked VIPs > 1.0 for A) *B.*
526 *meridionalis* and B) *S. laietanus* muscle lipidome comparing polluted sites (P1, P2, P3)
527 from reference sites (R1, R2, R3).
528
529 Figure 4. Heatmap cluster analysis of the lipidome of A) *B. meridionalis* and B) *S.*
530 *laietanus* from polluted sites (P1, P2, P3) *vs*. reference sites (R1, R2, R3). The color of
531 each section is proportional to the significance of the lipid change (red, increased levels;
532 green, decreased levels).
533
534 Figure 5. Volcano plots showing lipid significant differences between the lipidome of
535 A) *B. meridionalis* and B) *S. laietanus* from P sites *vs*. R sites with a fold change ≥ 2.0
536 and 1.5, and $p < 0.05$ *t*-test. Significantly altered lipids are coloured in red.

Figure 6. Boxplot of lipids selected as potential biomarkers of urban and industrial pollutants exposure for *B. meridionalis* and *S. laietanus* showing levels in reference and polluted sites. The box extends from 25th to 75th percentile; the horizontal bar within box is the median, whiskers represent 5-95th percentiles. *Significantly altered lipids ($p < 0.05$).

548 Figure 1.

549 A)

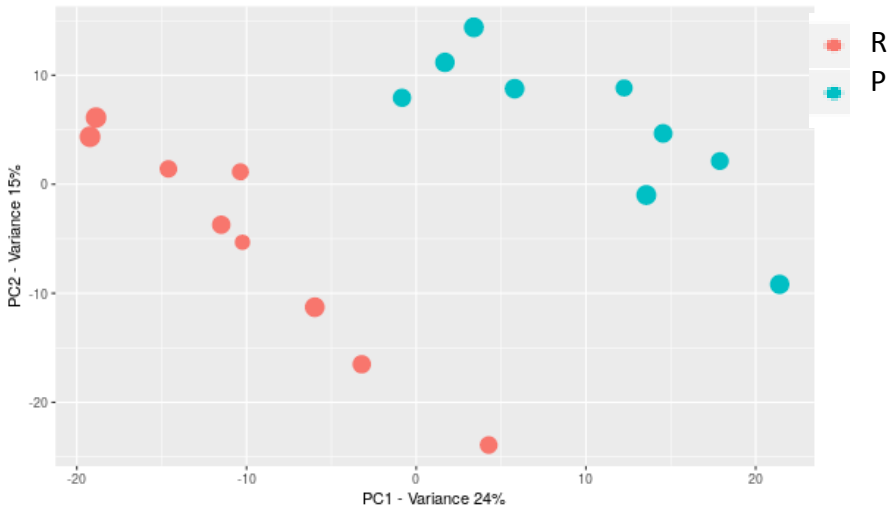

550

551 B)

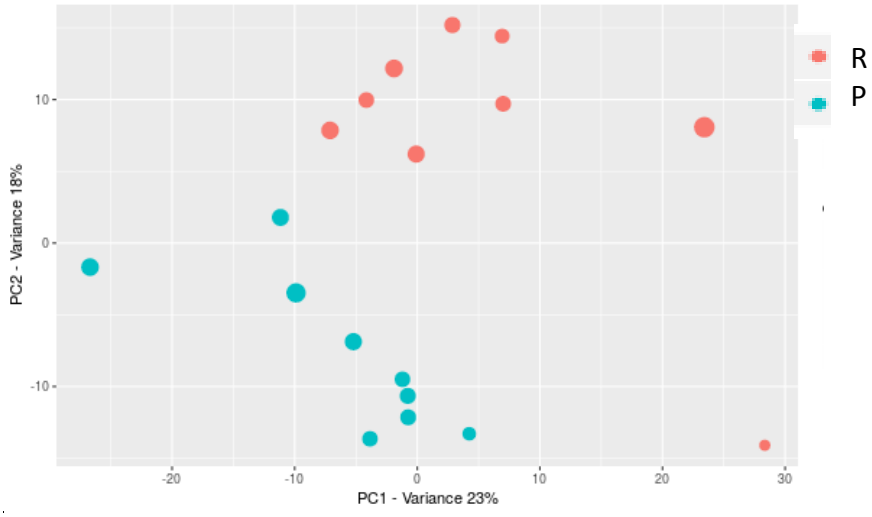

552

553

554

555

Figure 2.

A)

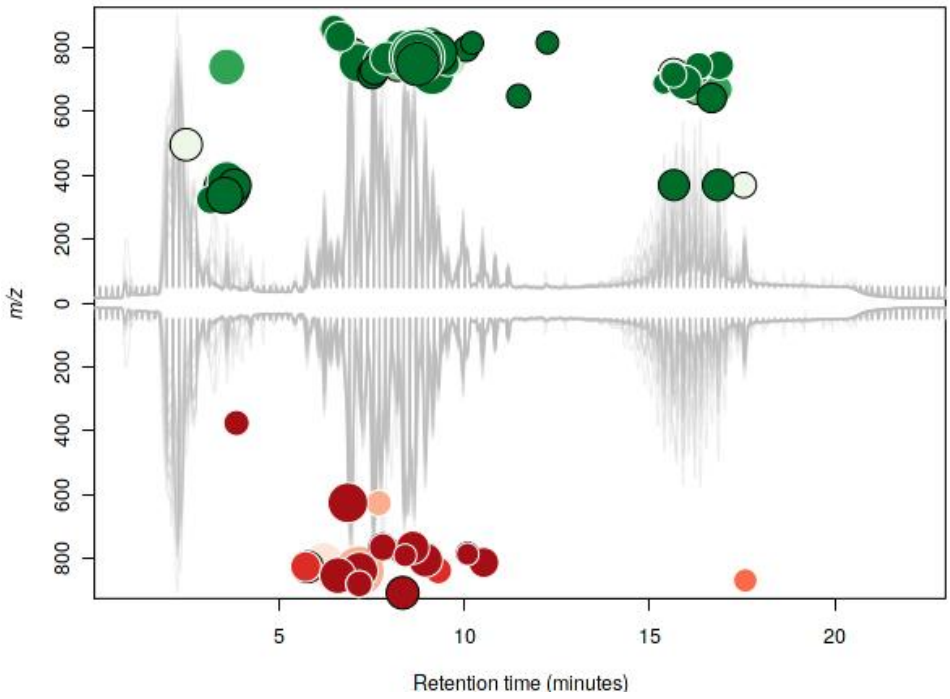
m/z
800
600
400
200
0
200
400
600
800
5
10
15
20
Retention time (minutes)

B)

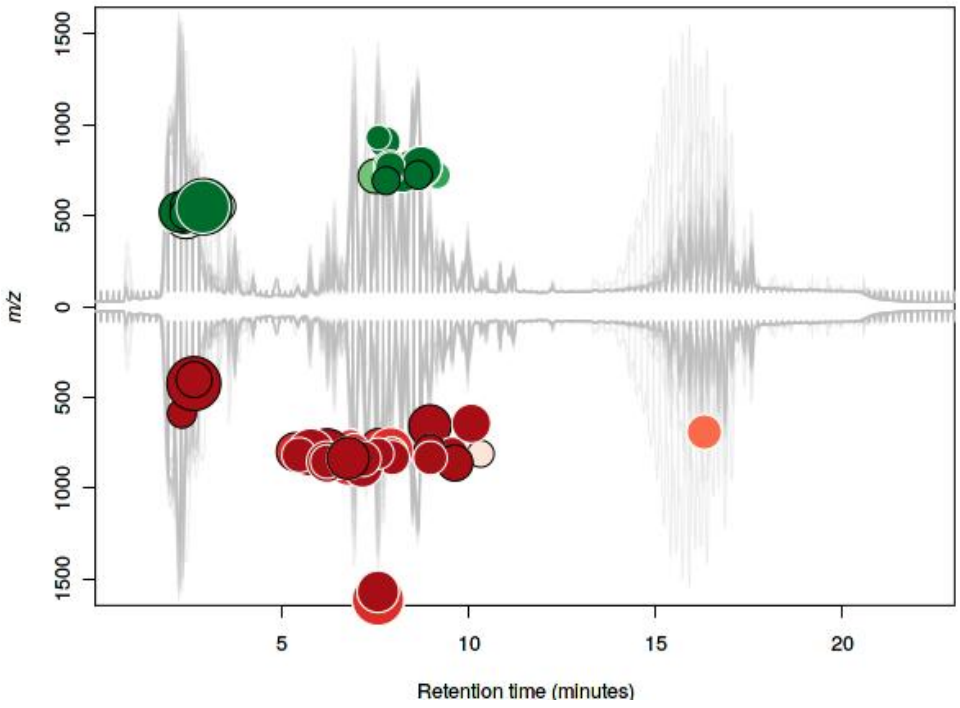
m/z
1500
1000
500
0
500
1000
1500
5
10
15
20
Retention time (minutes)

Figure 3.

A)

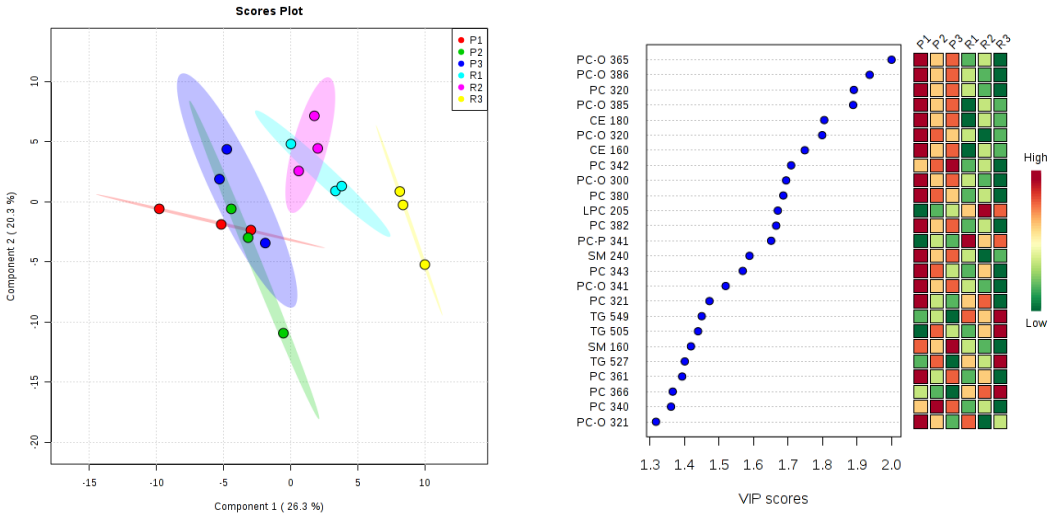
Scores Plot
P1
P2
P3
R1
R2
R3
Component 2 (20.3 %)
Component 1 (26.3 %)
PC-O 365
PC-O 386
PC 320
PC-O 385
CE 180
PC-O 320
CE 160
PC 342
PC-O 300
PC 380
LPC 205
PC 382
PC-P 341
SM 240
PC 343
PC-O 341
PC 321
TG 549
TG 505
SM 160
TG 527
PC 361
PC 366
PC 340
PC-O 321
High
Low
VIP scores

B)

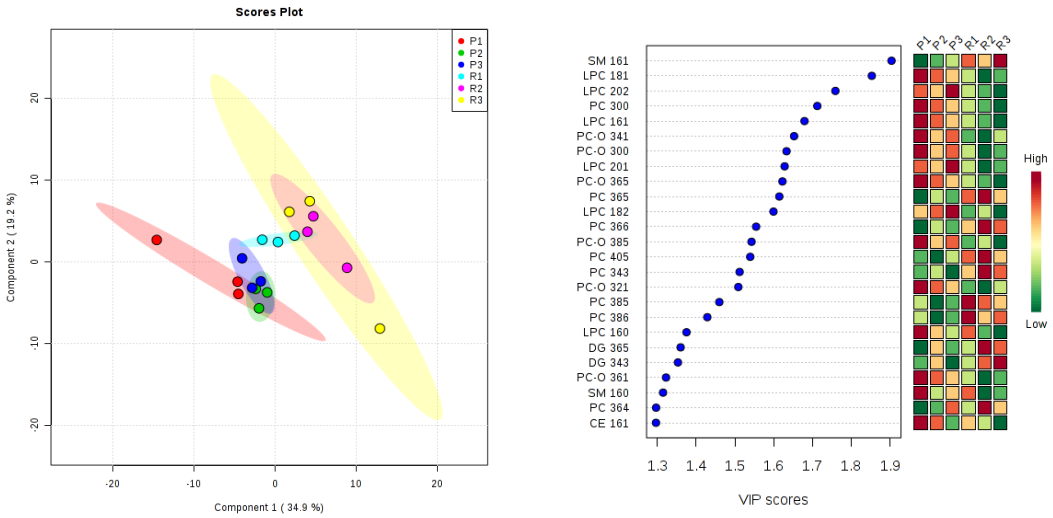
Scores Plot
P1
P2
P3
R1
R2
R3
Component 2 (19.2 %)
Component 1 (34.9 %)
SM 161
LPC 181
LPC 202
PC 300
LPC 161
PC-O 341
PC-O 300
LPC 201
PC-O 365
PC 365
LPC 182
PC 366
PC-O 385
PC 405
PC 343
PC-O 321
PC 385
PC 386
LPC 160
DG 365
DG 343
PC-O 361
SM 160
PC 364
CE 161
High
Low
VIP scores

Figure 4.

A)

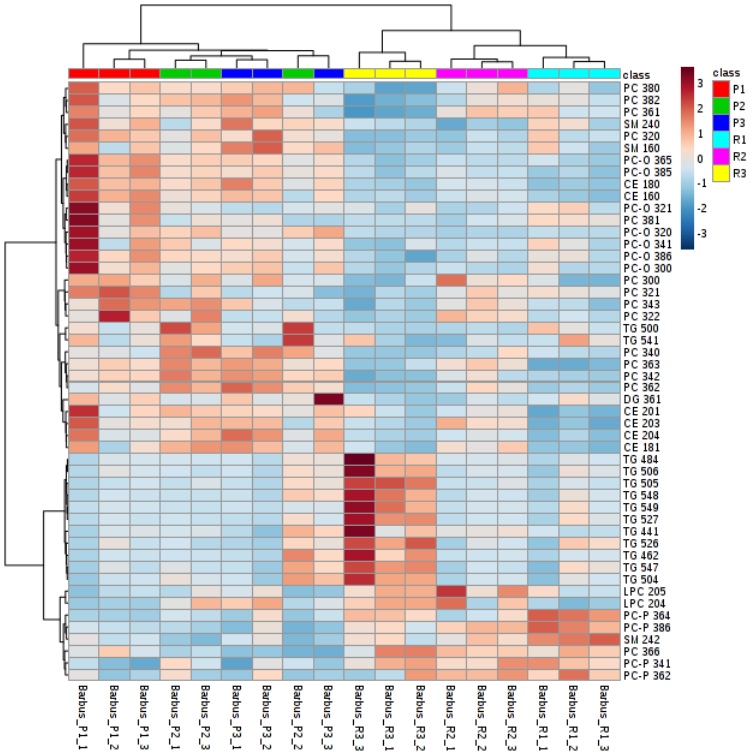
class
PC 380
PC 382
PC 361
SM 240
PC 320
SM 160
PC-O 365
PC-O 385
CE 180
CE 160
PC-O 321
PC 381
PC-O 320
PC-O 341
PC-O 386
PC-O 300
PC 300
PC 321
PC 343
PC 322
TG 500
TG 541
PC 340
PC 363
PC 342
PC 362
DG 361
CE 201
CE 203
CE 204
CE 181
TG 484
TG 506
TG 505
TG 548
TG 549
TG 527
TG 441
TG 526
TG 462
TG 547
TG 504
LPC 205
LPC 204
PC-P 364
PC-P 386
SM 242
PC 366
PC-P 341
PC-P 362
Barbus_P1_1
Barbus_P1_2
Barbus_P1_3
Barbus_P2_1
Barbus_P2_3
Barbus_P3_1
Barbus_P3_2
Barbus_P2_2
Barbus_P3_3
Barbus_R3_3
Barbus_R3_1
Barbus_R3_2
Barbus_R2_1
Barbus_R2_2
Barbus_R2_3
Barbus_R1_1
Barbus_R1_2
Barbus_R1_3
class
P1
P2
P3
R1
R2
R3
3
2
1
0
-1
-2
-3

B)

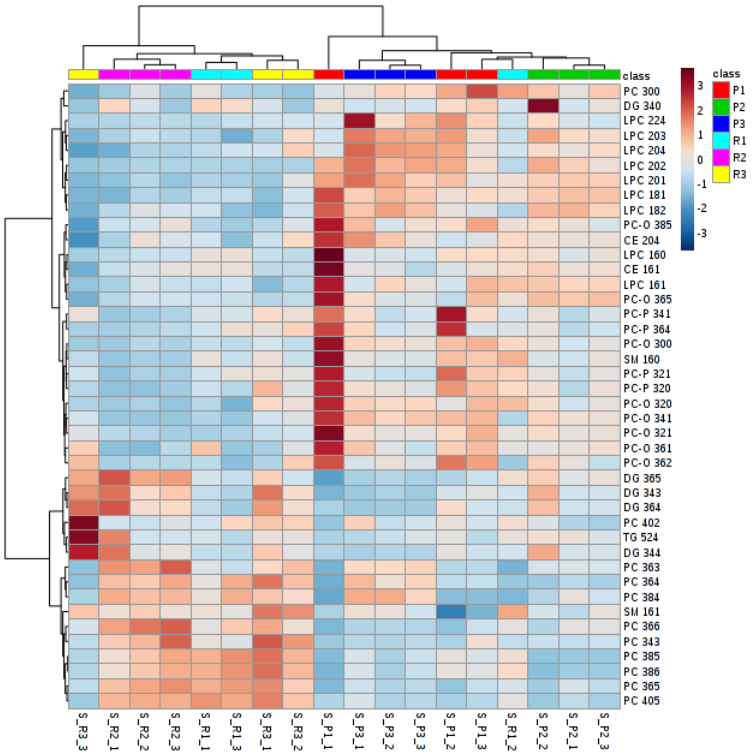
class
PC 300
DG 340
LPC 224
LPC 203
LPC 204
LPC 202
LPC 201
LPC 181
LPC 182
PC-O 385
CE 204
LPC 160
CE 161
LPC 161
PC-O 365
PC-P 341
PC-P 364
PC-O 300
SM 160
PC-P 321
PC-P 320
PC-O 320
PC-O 341
PC-O 321
PC-O 361
PC-O 362
DG 365
DG 343
DG 364
PC 402
TG 524
DG 344
PC 363
PC 364
PC 384
SM 161
PC 366
PC 343
PC 385
PC 386
PC 365
PC 405
S_R3_3
S_R2_1
S_R2_2
S_R2_3
S_R1_1
S_R1_3
S_R3_1
S_R3_2
S_P1_1
S_P3_1
S_P3_2
S_P3_3
S_P1_2
S_P1_3
S_R1_2
S_P2_2
S_P2_1
S_P2_3
class
P1
P2
P3
R1
R2
R3
3
2
1
0
-1
-2
-3

Figure 5.

A)

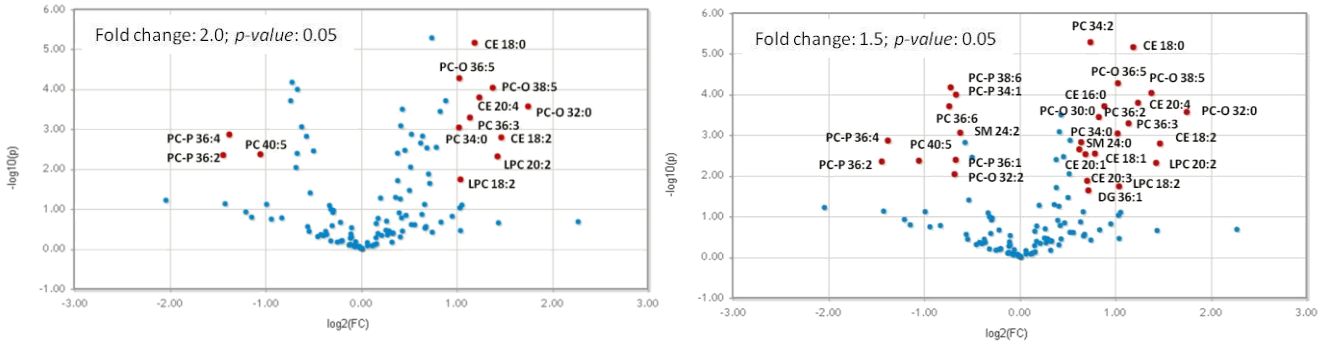
Fold change: 2.0; p-value: 0.05
CE 18:0
PC-O 36:5
PC-O 38:5
CE 20:4
PC-O 32:0
PC 36:3
PC 34:0
CE 18:2
LPC 20:2
LPC 18:2
PC-P 36:4
PC-P 36:2
PC 40:5
-log10(p)
log2(FC)
Fold change: 1.5; p-value: 0.05
PC 34:2
CE 18:0
PC-O 36:5
PC-O 38:5
PC-P 38:6
PC-P 34:1
CE 16:0
CE 20:4
PC-O 30:0
PC 36:2
PC-O 32:0
PC 36:6
PC 36:3
SM 24:2
PC 34:0
PC-P 36:4
SM 24:0
CE 18:2
PC 40:5
CE 20:1
CE 18:1
LPC 20:2
PC-P 36:2
PC-P 36:1
PC-O 32:2
CE 20:3
LPC 18:2
DG 36:1
-log10(p)
log2(FC)

B)

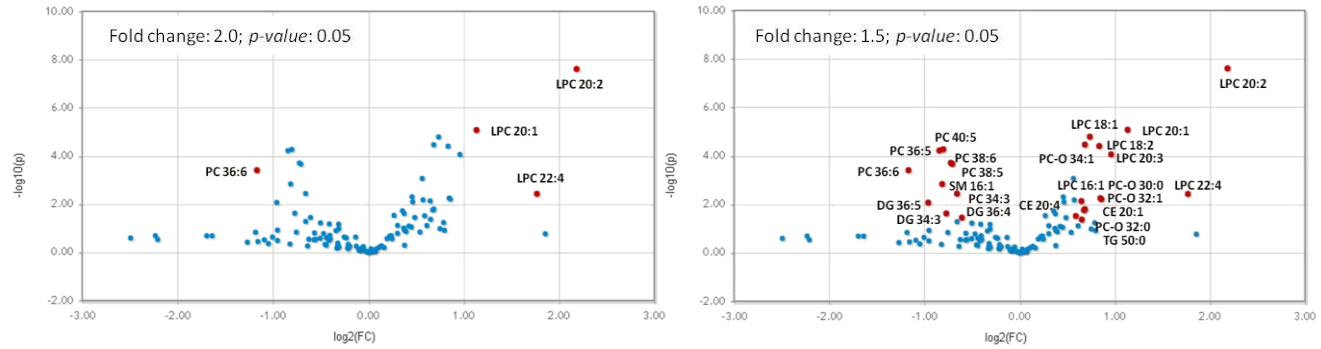
Fold change: 2.0; p-value: 0.05
LPC 20:2
LPC 20:1
PC 36:6
LPC 22:4
-log10(p)
log2(FC)
Fold change: 1.5; p-value: 0.05
LPC 20:2
LPC 18:1
LPC 20:1
PC 40:5
LPC 18:2
PC 36:5
PC 38:6
PC-O 34:1
LPC 20:3
PC 36:6
PC 38:5
SM 16:1
LPC 16:1
PC-O 30:0
LPC 22:4
PC 34:3
PC-O 32:1
DG 36:5
CE 20:4
DG 36:4
CE 20:1
DG 34:3
PC-O 32:0
TG 50:0
-log10(p)
log2(FC)

581 Figure 6.

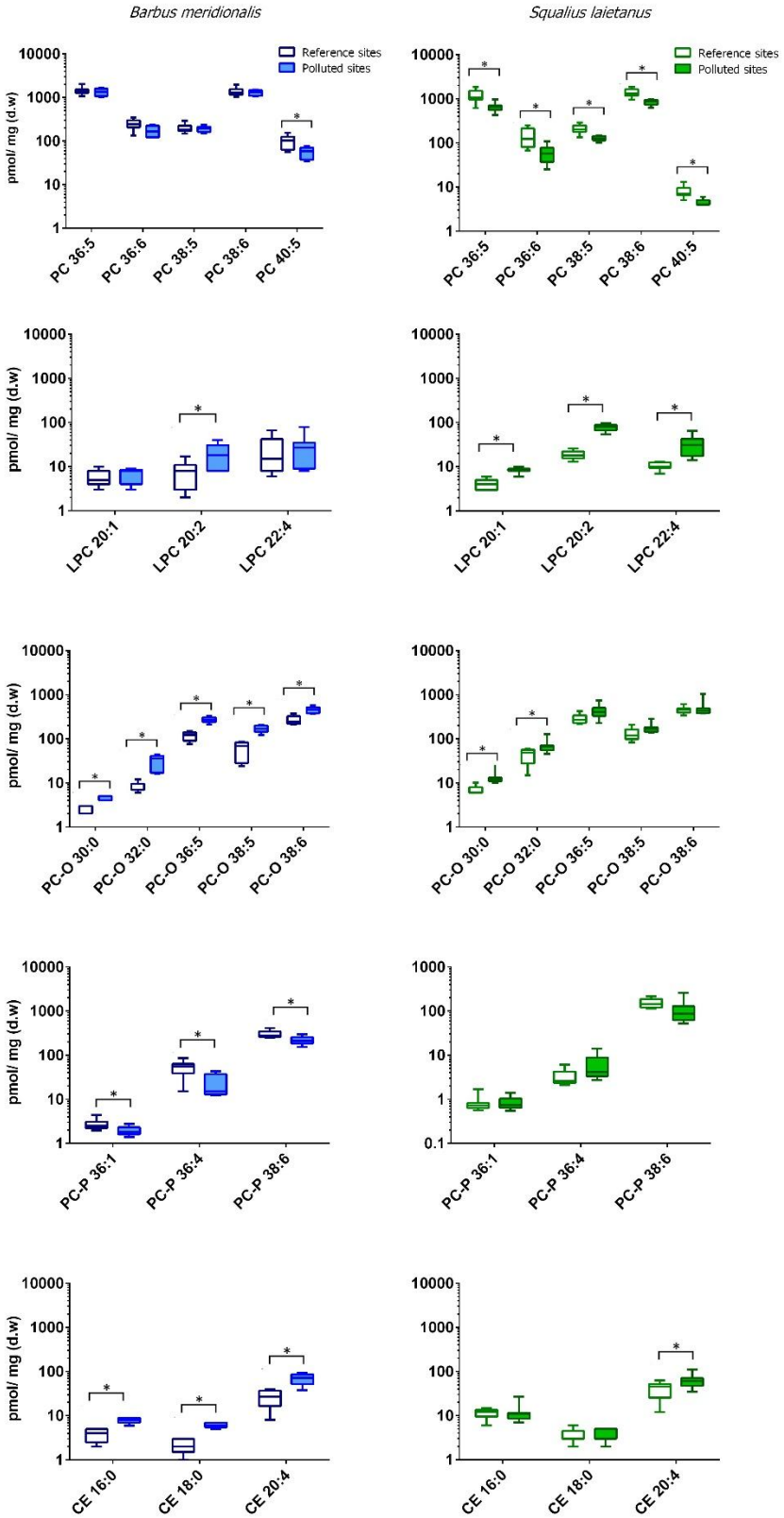

582

583

Supporting Information: Additional information on sampling (location and individuals), biliary levels of pollutants, a list of the lipid molecules detected in the skeletal muscle, and PCA analysis. An excel file containing the putative identifications from the untargeted analysis is also provided.